CArbon-14 Source Term

CAST

Final Report on Zr alloys corrosion studies at RWMC

(D3.19)

Author(s):

T. Sakuragi

Date of issue of this report: 21/12/2017

The project has received funding from the European Union's European Atomic Energy Community's (Euratom) Seventh Framework Programme FP7/2007-2013 under grant agreement no. 604779, the CAST project.		
Dissemination Level		
PU	Public	X
RE	Restricted to the partners of the CAST project	
CO	Confidential, only for specific distribution list defined on this document	

CAST – Project Overview

The CAST project (CArbon-14 Source Term) aims to develop understanding of the potential release mechanisms of carbon-14 from radioactive waste materials under conditions relevant to waste packaging and disposal to underground geological disposal facilities. The project focuses on the release of carbon-14 as dissolved and gaseous species from irradiated metals (steels, Zircaloys), irradiated graphite and from ion-exchange materials as dissolved and gaseous species.

The CAST consortium brings together 33 partners with a range of skills and competencies in the management of radioactive wastes containing carbon-14, geological disposal research, safety case development and experimental work on gas generation. The consortium consists of national waste management organisations, research institutes, universities and commercial organisations.

The objectives of the CAST project are to gain new scientific understanding of the rate of re-lease of carbon-14 from the corrosion of irradiated steels and Zircaloys and from the leaching of ion-exchange resins and irradiated graphites under geological disposal conditions, its speciation and how these relate to carbon-14 inventory and aqueous conditions. These results will be evaluated in the context of national safety assessments and disseminated to interested stakeholders. The new understanding should be of relevance to national safety assessment stakeholders and will also provide an opportunity for training for early career researchers.

For more information, please visit the CAST website at:
http://www.projectcast.eu

CAST		
Work Package: 2	CAST Document no. :	Document type:
Task: 3.3	CAST-2017-D3.19	R
Issued by: RWMC		Document status:
Internal no. :		Final

Document title
Final report on Zr alloys corrosion studies at RWMC

Executive Summary

RWMC has studied the aqueous corrosion of irradiated and unirradiated zirconium alloys under the simulated repository conditions. A sensitive hydrogen measurement technique (gas and absorbed) was selected to obtain the very low corrosion rate for unirradiated Zr alloys based on a reaction of $Zr + 2H_2O \rightarrow ZrO_2 + 2H_2$. Two experimental systems have been applied; the glass ampoule method, which is a batch type measurement under various types of solution and temperature, and the gas flow system which monitors the hydrogen gas continuously for a long term in a dilute NaOH solution of pH 12.5. In the corrosion tests for irradiated Zircaloy (spent BWR claddings), the concentrations of leached ^{14}C released as gaseous and dissolved organics and inorganics were measured together with other nuclides.

The equivalent corrosion rates obtained from total released ^{14}C (gaseous and dissolved) by assuming congruence with corrosion were less than that of unirradiated Zr alloys. Since this cannot be sufficiently explained with only the difference of the test condition (temperature), the congruence of ^{14}C leaching with corrosion is still unclear. The released ^{14}C from irradiated Zircaloy-2 under a pH of 12.5 was specified as gas and liquid phases. The gaseous ^{14}C fraction decreases with time. By contrast, the released fraction of ^{14}C in the liquid phase increased with time and reached over 90% after 2 years. The inorganic/organic partitions in the liquid phase were around 1/3 and seemed to be stable with time.

Instant release fraction (IRF) for spent claddings was also discussed through the experiment with the leached ^{14}C ratio from irradiated Zircaloy-2 having an oxide film and the ^{14}C inventory of the oxide part. The inventory measurement found that the abundance of ^{14}C in

the oxide was only 7.5%, which is less than the 20% commonly estimated in the safety case. Further, the leached ^{14}C from the irradiated cladding with oxide was found to be 0.0038% of the total ^{14}C activity after 6.5 years of immersion. These understandings should be reflected in the safety case that a lower IRF is justified or a negligible IRF is potentially suggested.

List of Contents

1   Introduction

The spent fuel cladding of light water reactors made of Zr alloys is expected to be disposed of in an underground repository (Figure 1). Carbon 14 (^{14}C) is a typical activated product in metallic wastes and is mainly generated by the ^{14}N(n,p)^{14}C reaction. For the waste in Japan as shown in Figure 2, it has been assumed that the Zircaloy hulls (spent fuel claddings) account for 80% by weight of the spent assembly waste, and their ^{14}C corresponds to 65.6% of the total ^{14}C inventory of 4.5×10^{14} Bq [SAKURAGI *et al.*, 2013]. The corrosion phenomenon is considered to be a leaching source of activated radionuclides such as ^{14}C and hydrogen gas. The corrosion behaviour of Zr alloys under anticorrosive repository conditions (low oxygen, highly alkaline, and temperature under 353 K) has been consequently outstanding, in large part because the corrosion rate is too low to be clearly measured by common methods [FRANKER and HARRIS, 1990]. Shoesmith and Zagidulin have reviewed the related papers and estimated that the corrosion rate of Zr alloys under repository condition is less than 1 nm/year [SHOESMITH and ZAGIDULIN, 2011]. Japanese safety case has estimated the corrosion rate of Zr alloys as 20 nm/year by measuring the evolved hydrogen gas of which 75 percent is assumed to be absorbed into the metal at 308 K, in the presence of 3,200 ppm chloride. This corresponds to its leaching periods of 11,400 years. [FEPEC and JAEA, 2007]. This Japanese report also mentioned that the above corrosion rate is concordant with the ^{14}C leaching rate from PWR cladding [YAMAGUCHI *et al.*, 1999]. The speciation of ^{14}C has been assumed to be an aqueous organic in this safety case. It is also the considerable impact on the safety case that the instant release fraction (IRF) for the spent fuel cladding (Zircaloy hull) is assumed to be 20% of the total ^{14}C inventory, which is regarded as the inventory of the oxide layer [FEPEC and JAEA, 2007].

The purpose of this report is to investigate the corrosion behaviour of unirradiated Zr alloys, and irradiated Zr alloys (fuel claddings). The instant release fraction (IRF) for hull waste was also discussed through the experiments with irradiated Zircaloy having an oxide layer. The long-term corrosion behaviour of the Zircaloy-2, Zircaloy-4 and pure Zr under deoxygenated conditions has been performed by hydrogen gas and absorbed hydrogen

measurements. A high pH solution (NaOH) was selected to simulate the typical underground repository environment, and deionized water and other types of solution were selected to understand fundamentally the factors affecting the corrosion behavior. We have employed two experimental setups to measure sensitively the hydrogen gas from the corrosion reaction that can be applied to the extremely low corrosion rate of Zr alloys. The batch ampoule method was applied to relatively short-term tests and for the tests in various conditions. The gas flow experiment that can monitor the evolved hydrogen continuously was applied to a long-term behaviour.

The corrosion test using irradiated Zircaloy-2 (spent BWR cladding) by measuring the released ^{14}C has been performed in a dilute NaOH solution (pH 12.5) at room temperature. The concentrations of released ^{14}C as gas and dissolved organics and inorganics were measured. The equivalent corrosion rates obtained from total released ^{14}C (gaseous and dissolved) by assuming congruence with corrosion were also determined.

The instant release fraction (IRF) for hull waste was also discussed through the experiments. The release of radionuclides from the metal matrix is regarded as the corrosion-related congruent release. Conversely, the oxide film formed on the Zircaloy cladding surface is regarded as a source of IRF. Guenther et al. [GUENTHER *et al.*, 1990] and Yamaguchi et al. [YAMAGUCHI *et al.*, 1999] studied the external oxide layer formed by in-pile corrosion of irradiated Zircaloy fuel cladding and estimated that the total ^{14}C contained in the layer is about 15% (Guenther) or 17% (Yamaguchi). Sakuragi et al. [SAKURAGI *et al.*, 2013] have employed the ORIGEN calculation using the chemical composition and oxide thickness of Japanese cladding to estimate the ^{14}C inventory of the oxide layer as approximately 9% for PWR hulls and 0.8% for BWR hulls. We have prepared an irradiated Zircaloy-2, with an external oxide film 25.3 μm thick. The content of ^{14}C was determined by a wet chemical treatment and liquid scintillation counting of ^{14}C activity using different parts of the cladding such as the base Zircaloy metal, oxide, and metal with and without oxide film. A static leaching test using cladding tube , for which the internal oxide was removed, was carried out for an exposure period of 6.5 years.
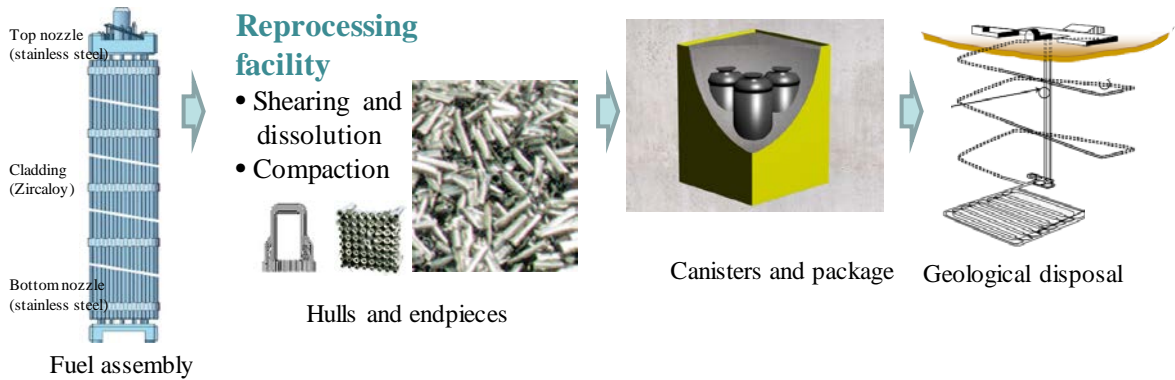
Figure 1 Generation and disposal concept of activated metallic waste in Japan.
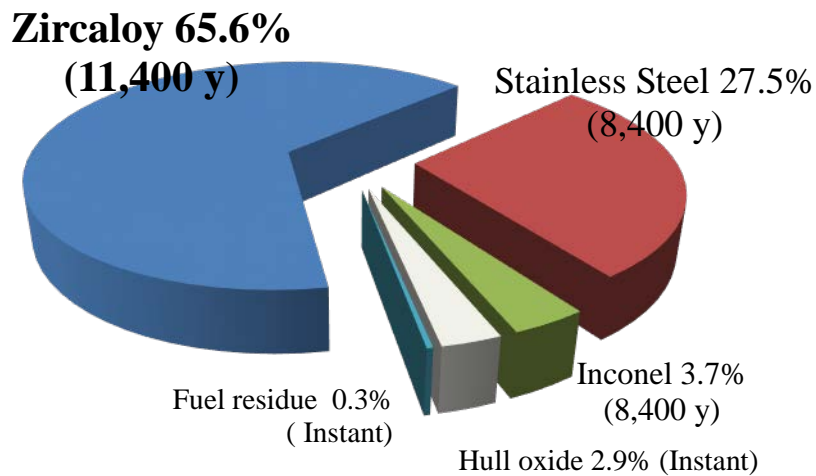
Figure 2 ^{14}C inventory for spent fuel assemblies corresponding to commercial 32,000 MTU reprocessing in Japan [SAKURAGI et al., 2013]. The values in parentheses represent the assumed leaching period in the Japanese safety assessment [FEPEC and JAEA, 2007].

2 Corrosion Test of unirradiated Zr Alloys

2.1 *Experimental*

2.1.1 Specimen

Zircaloy-4, Zircaloy-2 and pure zirconium obtained from CEZUS Co., Ltd. were pretreated to produce a sample of appropriate thickness by undergoing two sets of cold-rolling, followed by vacuum annealing after each set to remove the hydrogen absorbed during cold-rolling. The accumulated annealing parameter before purchase is not known. Final polishing was done with 0.02 mm alumina powder. The initial hydrogen content was lower than 10 ppm, as shown together with other elements in Table 1. Figure 3 shows the surface observation of Zircaloy-4 before the corrosion test, by using by transmission electron microscopy (TEM). The initial oxide thickness was approximately 5 nm.

Table 1 Chemical compositions of Zr alloys (wt%)

|	Sn	Fe	Cr	Ni	O	H	N
Zircaloy-4	1.24	0.18	0.10	< 0.006	0.15	0.001	0.003
Zircaloy-2	1.23	0.13	0.10	0.04	0.13	0.0004	0.002
Zirconium	< 0.006	0.04	< 0.006	< 0.006			
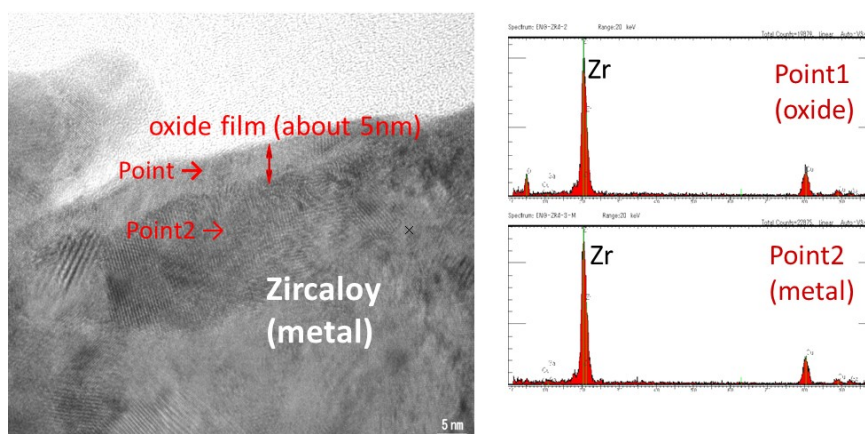
Figure 3 Surface observation of Zircaloy-4 by TEM observation (right) and EDX analysis (left) before immersion.

4

2.1.2 Batch Ampoule Experiment

Corrosion test was performed by an ampoule batch method developed by Honda et al. [HONDA *et al.*, 1999], and the test procedure is presented in Figure 4. Zirconium and alloys specimen of 23 strips (21 pieces; 3 mm×90 mm×0.1 mm, 2 pieces; 3 mm×90 mm×0.05 mm) were placed in a glass ampoule. The absorbed hydrogen will be measured for the thin strips (0.05 mm) after gaseous hydrogen measurement described in section 2.1.4. A stop-cock was attached, then the ampoule was filled with an appropriate solution mentioned below and the stop-cock closed. This enclosure procedure was performed in a glove box (see Figure 5) that had been purged by nitrogen gas with oxygen concentration below 0.1 ppm. The ampoules were moved outside the glove box and sealed by heating. After corrosion, the ampoules were set on the vacuum gas collecting system connected with a gas chromatography (YANACO G-2800) and hydrogen gas was measured.

The test solutions were deionized water, dilute NaOH solution adjusted to pH 12.5, $Ca(OH)_2$ solution close to saturation of pH slightly less than 12.5, and cement water which simulates ground water equilibrated with seawater and OPC cement prepared from reagents (Table 2) .
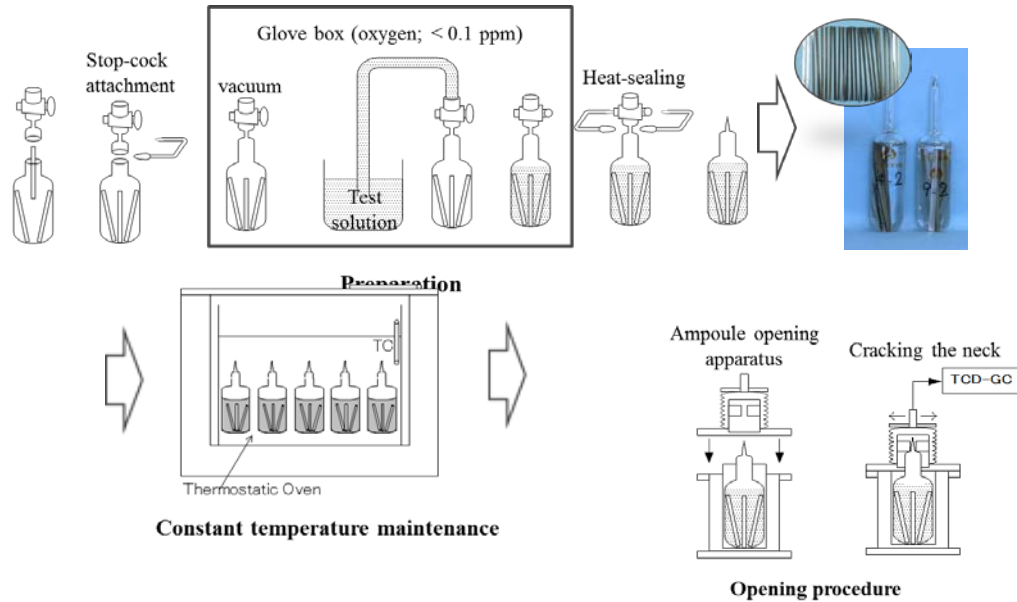
Hydrogen analysis method
 Gas phase
   - **Released Hydrogen Gas : Gas chromatography ((TCD-GC)**
 Test Specimen
   - **Absorbed hydrogen: Inert gas melting system* coupled with gas chromatography**
   - **Characteristics of oxide film: TEM-EDX, Electron diffraction, XPS**

* high-frequency induction heating ~ 2000C

Figure 4 Procedure for ampoule batch corrosion experiment.

Figure 5 Glove box for preparation of glass ampoule.

Table 2 Chemical compositions of cement water (mol/dm^3)

| pH	Na$^+$	Ca^{2+}	SiO$_2$	Al^{3+}	Cl$^-$	SO$_4^{2-}$	HCO$_3^-$/CO$_3^{2-}$
12.5	6.0×10^{-1}	2.8×10^{-2}	3.0×10^{-5}	7.7×10^{-6}	6.0×10^{-1}	2.4×10^{-4}	1.4×10^{-5}

2.1.3 Gas Flow Experiment

The experimental setup for the gas flow corrosion system is shown in Figure 6. This system can monitor the generated hydrogen gas continuously. The Zr alloy samples (100 sheets; 100 mm×100 mm×0.1 mm, surface area of 2.0 m^2) were immersed in 2.5 dm^3 of deoxygenated deionised water or dilute NaOH solution (initial pH = 12.5). An argon carrier gas was passed through the inner flask, and the hydrogen concentration in the carrier gas was measured periodically using atmospheric pressure ionization mass spectrometry (API-

MS, Hitachi Tokyo Electronics, UG-400). Hydrogen contamination from the atmosphere (approximately 0.5 ppm) and also oxygen was avoided by using a double container system. Several test vessels were prepared together with a vessel of a blank test and for hydrogen absorption measurements.

The cumulative atomic molar amount of gaseous hydrogen per unit surface area, A_{gas} (mol/m^2), can be obtained from

$$A_{gas} = \frac{2}{S_g} \sum \frac{C_{t_i} + C_{t_{i-1}}}{2} \cdot \frac{v}{V°} \cdot (t_i - t_{i-1}), \qquad (1)$$

where C_{ti} is the concentration of hydrogen gas (H$_2$) at time t_i, t_{i-1} is one time increment before t_i, v is the gas flow rate of the carrier gas (0.9 dm^3/min.), V° is the molar volume of a perfect gas (22.4 dm^3/mol), and S_g is the surface area (2.0 m^2).
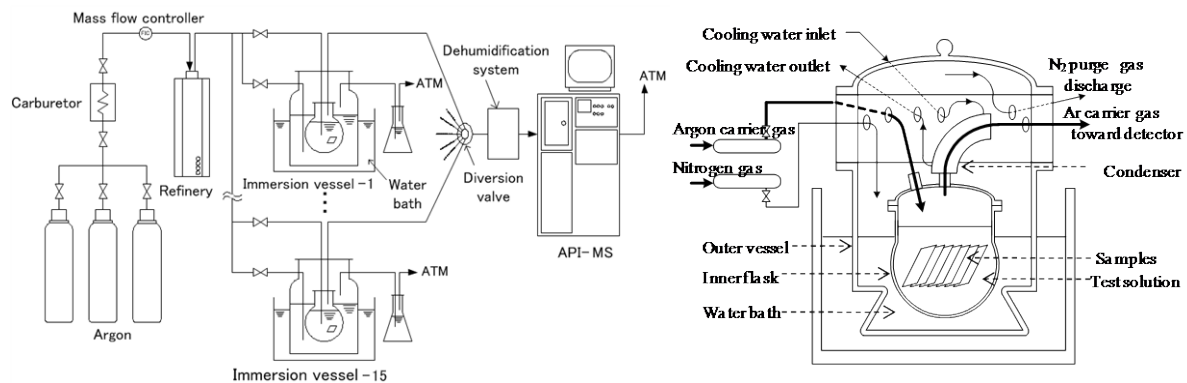
Figure 6 Overview of the gas flow experimental system (left) and detailed illustration of the immersion vessel (right).

2.1.4   Absorbed Hydrogen Measurement

The hydrogen contents in Zr alloys were determined by the inert gas melting system coupled with gas chromatography (LECO RH-404) in accordance with Japanese Industrial Standard Z 2614, as the following procedure.

· After the corrosion experiment, the Zr alloy samples (strip; 3 mm×90 mm×0.05 mm, 0.12 – 0.15 g) were collected from the test solution.

· The strip was rinsed with deionized water, dried and kept in a vacuum desiccator to avoid water adsorption before use.

· The strip was cut finely and placed in a graphite crucible together with Tin as a fusing agent.

· The graphite crucible was heated rapidly to 2273 K by an AC impulse furnace, and the gas components in melt were discharged under a constant flow of Ar carrier gas.

· Carbon species in the carrier gas was removed by a NaOH absorber after oxidized monoxide to carbon dioxide by passing through a glass cell packed with iodine pentoxide (I_2O_5) at room temperature.

· Hydrogen was fractionated using a gas chromatography (Molecular Sieve) and determined using a thermal conductivity detector.

· This analytical system is calibrated using the standard Zr metal (ALPHA Resources INC.) of which hydrogen contents are known in the range of 10 to 20 ppm.

The system is shown in Figure 7. The initial hydrogen content was measured below 10 ppm before the corrosion test. The very thin sample (0.05 mm thick) was used for the absorption measurement to increase the hydrogen concentration by increasing the specific surface area.

The molar amount of hydrogen absorbed in Zircaloy metal per unit surface area A_{abs} (mol/m^2) is given by (2).

$$A_{abs} = \frac{H_{abs} \cdot W \cdot 10^{-6}}{M_H \cdot S_a}, \qquad (2)$$

where H_{abs} is absorbed hydrogen in ppm, W is the sample weight, M_H is the molecular weight of hydrogen (1 g/mol), and S_a is the surface area (strip sample; $1.2×10^{-3}$ m^2).
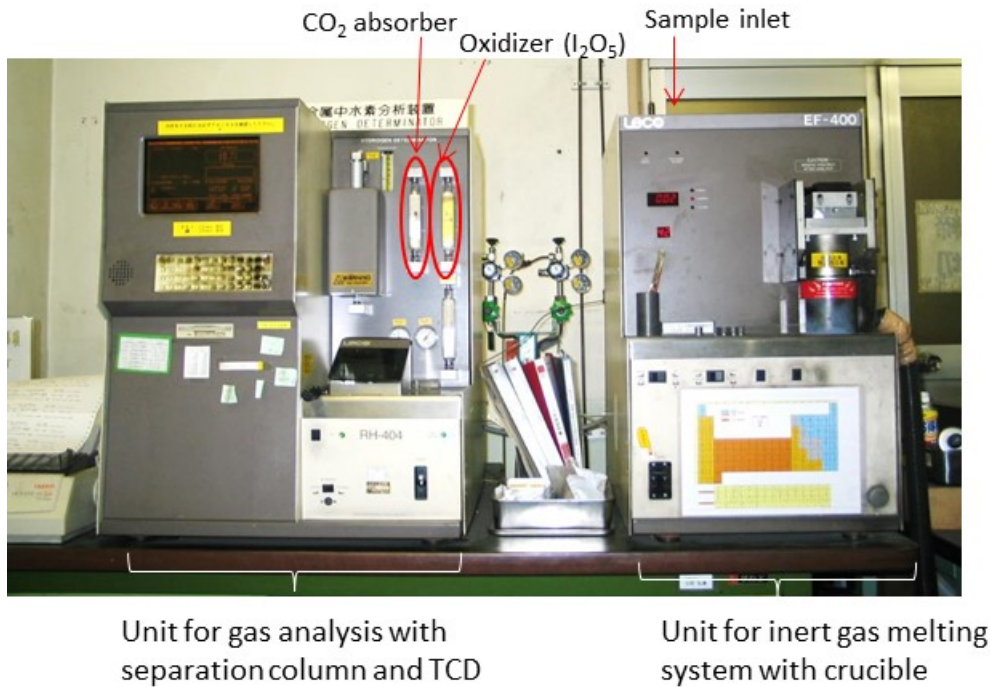
Figure 7 Inert gas melting system coupled with gas chromatography (LECO RH-404) for absorbed hydrogen measurement.

2.2 *Corrosion Rate*

The corrosion rate for unirradiated Zr alloys can be obtained from the total amount of generated hydrogen (gas and absorbed), based on the following reaction:

$$Zr + 2H_2O \rightarrow ZrO_2 + 2H_2 \qquad (3)$$

Based on the oxidation reaction under stoichiometry in equation (3), the corrosion rate, R_c (nm/y), is obtained from the following equation.

$$R_c = \frac{(A_{gas} + A_{abs}) \cdot M_{Zr}}{4 \cdot \rho_{Zr} \cdot t} \cdot 10^9 \qquad (4)$$

where A_{gas} and A_{abs} are the molar amount of hydrogen gas and absorbed in Zircaloy metal per surface area unit (mol/m^2), respectively, as mentioned in the previous sections, M_{Zr} is the molecular weight of zirconium (91.22 g/mol), ρ_{Zr} is the zirconium density (6.44×10^6 g/m^3), and t is the test time (years).

The corrosion rate for irradiated Zircaloy-2 was obtained from the released ^{14}C using BWR cladding without oxide film immersed in a dilute NaOH solution of pH 12.5 and nitrogen atmosphere at room temperature around 293 K. Detailed experiments are described in the following section (Section 3. Corrosion Test of Irradiated Zr Alloy). ^{14}C in gas and aqueous phase was measured by liquid scintillation counting (LSC). Assuming that the activated ^{14}C is distributed homogeneously in the cladding, the equivalent corrosion rate, R_{eq}, can be obtained from

$$R_{eq} = \frac{aL}{2At} \tag{5}$$

where, a is the leached amount of ^{14}C (Bq), A is the inventory in the cladding (Bq), L is the thickness of the cladding (nm), and t is the test time (years).

Figure 8 shows the results of the corrosion rate for unirradiated Zircaloys and the equivalent corrosion rate for irradiated Zircaloys. The solid lines represent the corrosion rate obtained from the following high temperature corrosion equation (6) and (7) by Hillner [HILLNER, 1977],

$$\Delta W^3 = k_C \times t \tag{6}$$

$$k_C = 365 \times 6.36 \times 10^8 \exp(-13636/T) \tag{7}$$

$$R_c = \frac{10^9 \cdot M_{Zr}}{2 \cdot M_O \cdot \rho_{Zr} \cdot t} \cdot \left(k_c \cdot t\right)^{1/3} \tag{8}$$

where ΔW is the weight gain (g/m^2), k_C is the cubic rate constant (g^3 m^{-6} y^{-1}), t is the time (year), T is the temperature (K), and M_{Zr} is the molecular weight of oxygen (16.0 g/mol). The difference between the extrapolation of high temperature corrosion and the corrosion

rates for the present work is remarkable as the temperature decreases. This indicates the corrosion kinetics at high temperature and low temperature are not strictly the same.

The corrosion rate decreases with time and increases with the temperature. There is no difference of corrosion rate between Zr, Zircaloy-2 and Zircaloy-4. Other factors are not significant at temperatures above 323 K. Figure 9 shows the data obtained at 303 K at higher magnification. The corrosion rates in the ampoule tests show slightly larger corrosion rates than that obtained by the gas flow system. This difference in results according to the experimental method was also observed for the corrosion of stainless steel [SAKURAGI, WP2 report (D2.12)]. This reason is currently unknown, but generally, unpolished metals show a trend of rapid corrosion. This result may be attributed to the fact that the surface area of the unpolished edge was a larger ratio of the specimen area for the batch ampoule test (thin strips) than for the gas flow test (100 mm square foils). In the ampoule tests, the corrosion rate of Zircaloy-4 in the cement water (see Table 2) is higher than Zircaloys in NaOH solution and Zr in pure water. It may be suggested that a part of component such as chloride ion influences the corrosion rate, but the pH and temperature seem to be the key parameter affecting the corrosion rate.

The equivalent corrosion rate of irradiated Zircaloy is less than that of unirradiated Zircaloy, a part of which is attributed to the temperature. However, the congruence of ^{14}C leaching with corrosion has not been confirmed yet and is one of the most important challenge for future.
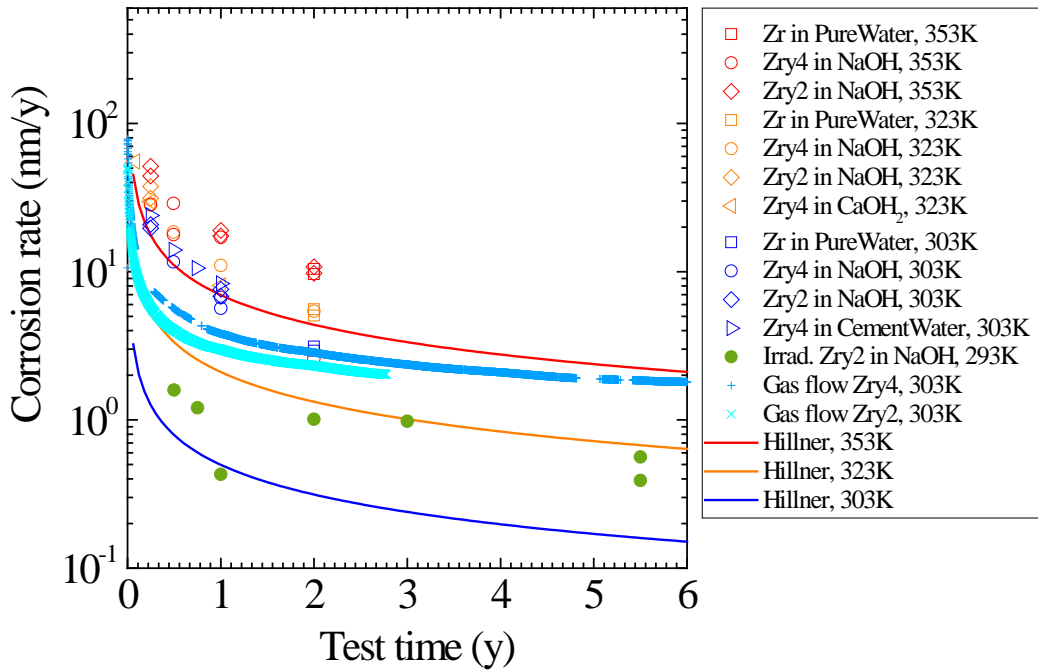
Figure 8 Corrosion rate for the unirradiated Zr alloys by the glass ampoule method under various conditions together with the corrosion rate by gas flow system [SAKURAGI et al., 2013], the equivalent corrosion rate for irradiated Zircaloy-2 (BWR cladding without oxide) obtained from leached ^{14}C, and the corrosion rate obtained from the Hillner equation [HILLNER, 1977] at any temperatures.
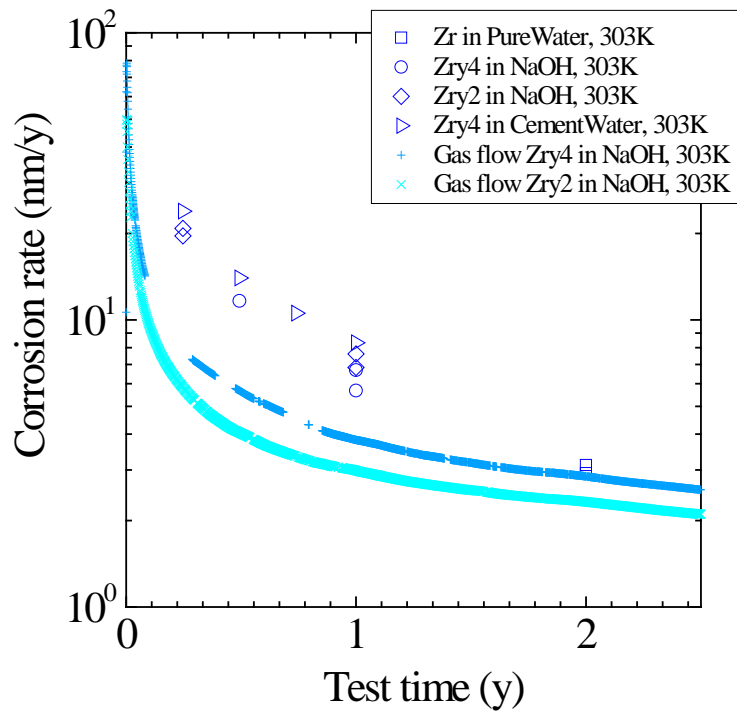

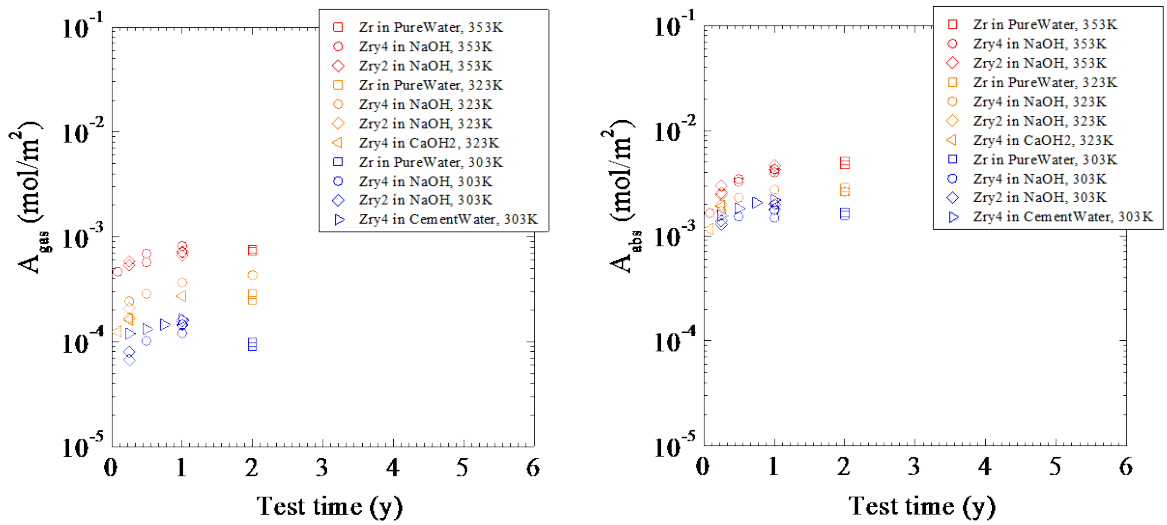**Figure 9 Corrosion rate of unirradiated Zr alloys at 303 K**

2.3 *Hydrogen Pick-up Ratio*

The hydrogen absorption behaviour into Zr alloys is of importance for estimating the corrosion rate, hydride formation, and the gas loading on a disposal facility system. This section discusses the hydrogen absorption during aqueous corrosion.

The hydrogen pick-up ratio x can be defined as

$$x = \frac{A_{abs}}{A_{gas} + A_{abs}} , \qquad (9)$$

where A_{gas} and A_{abs} are the atomic molar amount of gaseous hydrogen and absorbed hydrogen in Zircaloy metal per surface area unit (mol/m^2), respectively, as mentioned in the previous sections. Figure 10 shows the A_{gas} and A_{abs} in the ampoule corrosion tests. The values of A_{gas} are smaller than that of A_{abs}. Figure 11 shows the pick-up ration as a function of test time. The pick-up ratio increases rapidly with time and is approximately constant in the long term at very high percentages as around 95% for 303 K, 90% at 323 K, 85% for 353 K, respectively. Generally, the hydrogen pick-up ratio into cladding during operation of nuclear power plants is known to be 2.5-20% for BWR (around 280°C) and 10-20% for PWR (around 320°C), respectively. The amazing results of high pick-up ratios in the present work might be justified in the results for stainless steel corrosion because the pickup ratio into stainless steel obtained in the same manner as Zr alloys was less than 3% [SAKURAGI *et al.*, 2016 a]. The temperature dependence of the pick-up ratio together with the general in-pile results for BWR and PWR is shown in Figure 12, indicating that the hydrogen pick-up ratio into Zr alloys decreases with rising temperatures. Assuming that the hydrogen absorption process occurs after sorption of atomic hydrogen onto a surface (metal or oxide), the temperature dependence of pick-up ratio is sensible because the higher temperature shall make the sorption to be harder. Furthermore, it can be speculated that the gasification rate exceeds the duration of hydrogen adsorbed on the surface when the hydrogen supplied by the cathodic water decomposition is rapid.

Figure 10 Hydrogen gas generation (left) and absorption (right) for the unirradiated Zr alloys by the glass ampoule corrosion tests.
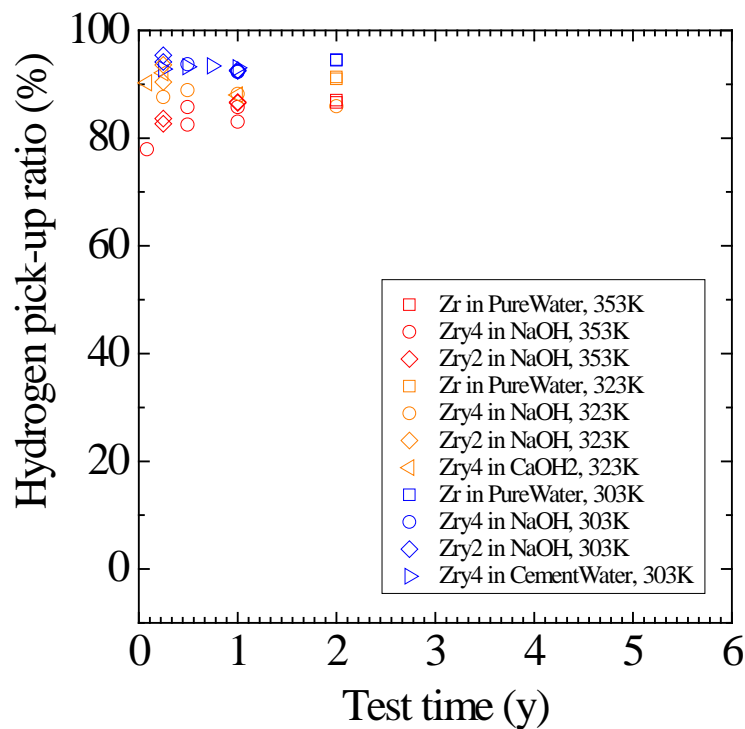
Figure 11 Hydrogen pick-up ratio for the unirradiated Zr alloys by the glass ampoule corrosion tests as functions of time.
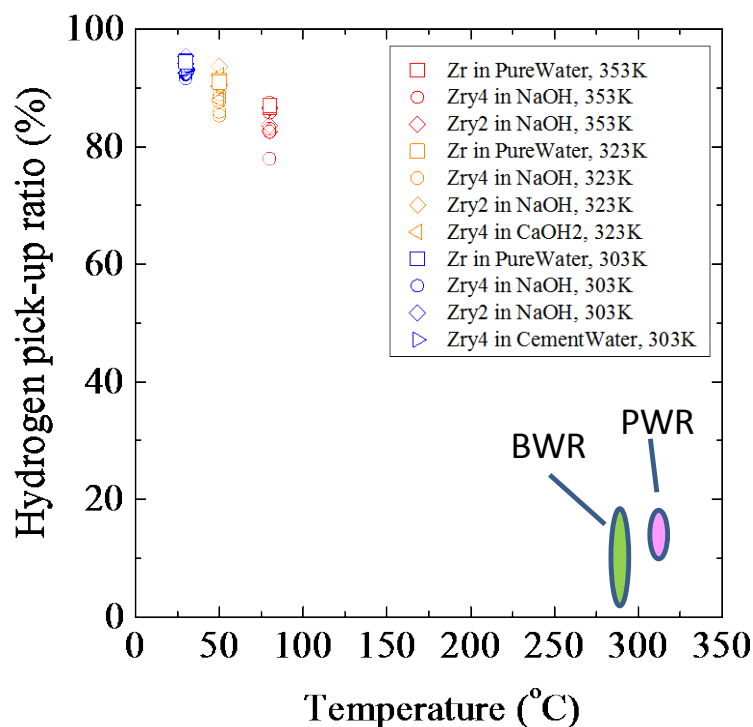
Figure 12 Hydrogen pick-up ratio for the unirradiated Zr alloys by the glass ampoule corrosion tests as functions of temperature.

2.4 *Surface characterisation of the oxide*

Figure 13 show the surface analyses of corroded Zircaloy-4 at different temperatures in dilute NaOH solution of pH 12.5, respectively. The oxide film thickness increases with increasing temperature. It is approximately 7 nm at 30°C, 10 nm at 50°C, and 14 nm 80°C according the TEM observations. The XPS analysis also demonstrated the increase of oxide thickness with temperature. The crystallization of the oxide is shown by electron diffractions. The tetragonal structure is likely to be formed. This passive film may control the corrosion. However, the monoclinic structure which is stable and found for the oxide formed in the plant operation temperature is not confirmed in this diffraction.
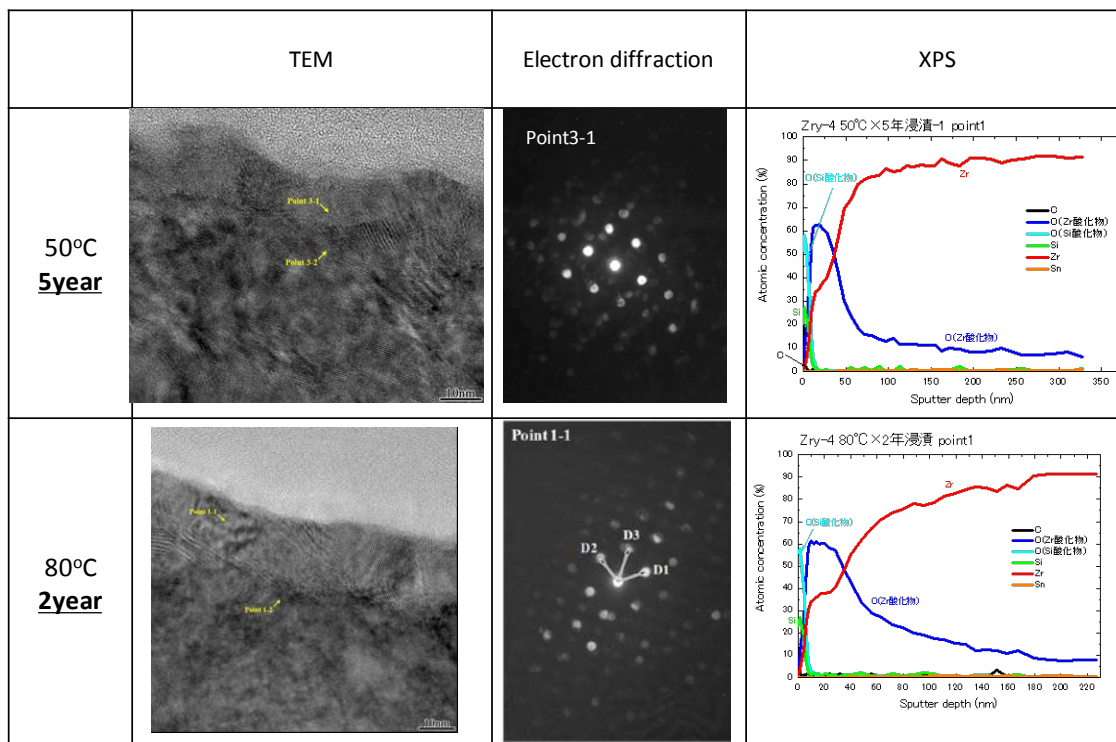
**Figure 13 Oxide film measurements in NaOH solution (pH 12.5).**

3   Corrosion Test of Irradiated Zr Alloy

3.1 *Irradiated Zircaloy-2*

The corrosion tests following inventory measurements for irradiated Zr alloy have been performed using spent Zircaloy-2 cladding from a BWR fuel rod. We prepared two types of BWR fuel cladding; a STEP I type fuel is an older fuel type in Japan that uses an 8×8 array in a lattice configuration (general burnup of 33 GWd/t), and a STEP III type fuel is relatively new fuel type that uses an 9×9 array (general burnup of 45 GWd/t). Table 3 presents the characteristics and specific irradiation condition of the irradiated Zircaloy-2. The claddings were prepared by a procedure shown in Figure 14. After their removal, the claddings were washed with 4 M of HNO_3 in a warm bath and cut to an appropriate size. Figure 15 shows the appearance of the cladding. The thickness of the surface oxide layer was measured based on the micrography as shown in Figure 16.

Table 3 Characteristics of irradiated Zircaloy-2

Fuel Type	Material	Burnup (GWd/t)	Cycles	Outer oxide thickness (average, μm)
BWR STEP I	Zircaloy-2	41.6	5	19.9
BWR STEP III	Zircaloy-2	39.7	3	2.7
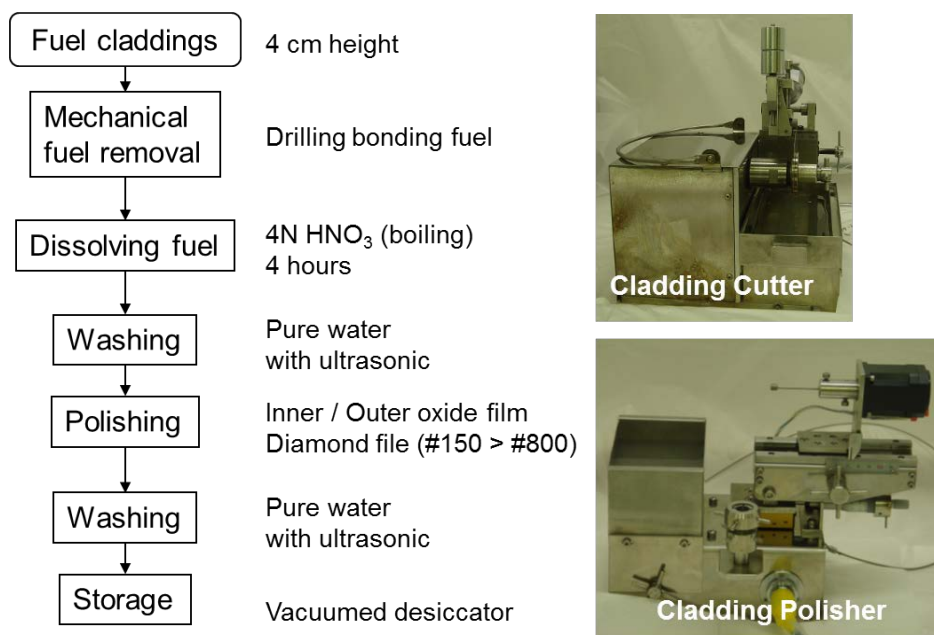
Figure 14 Pretreatment procedure for irradiated Zircaloy-2 for inventory measurement and corrosion test.

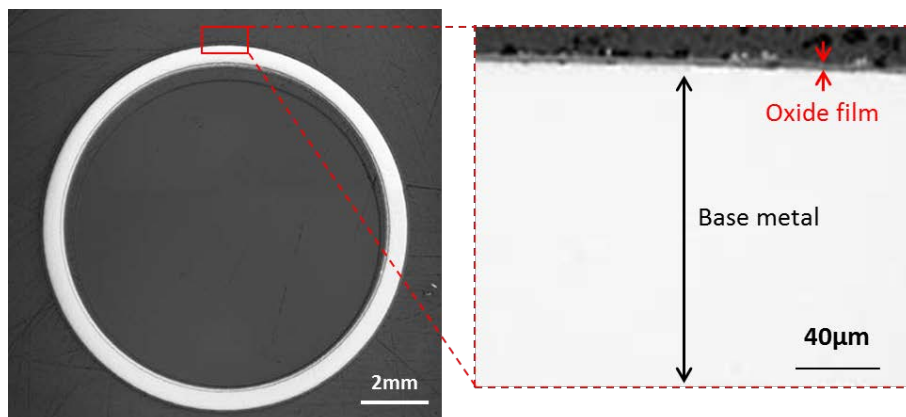**Figure 15 I**rradiated Zircaloy-2 (BWR STEP III) after HNO$_3$washing.

Figure 16 SEM images for irradiated Zircaloy-2 (BWR STEP III) before corrosion test.

3.2 ^{14}C Inventory Measurement

Figure 17 presents the analytical procedure to measure the inventory for irradiated Zircaloy-2. The inventory measuring apparatus is also shown in Figure 18. The digestion process by a mixed acid of nitric acid and fluoric acid generates two types of samples: gas and liquid samples. The gas emitted at the time of the sample digestion was drawn in the recovery line, which consists of an iodine trap, a cold trap, an alkaline trap, and collected ^{14}C. The potential contamination by radioiodine in a volatile state was removed by an AgI precipitation. The liquor of digestion was recovered, and gamma nuclides activities were

measured by the germanium semiconductor detector. Carrier and oxidizer and catalyst were supplied to the remaining solutions, wet oxidation of the remains organic matter was carried out, and ^{14}C was collected in the three steps of an alkaline trap. The ^{14}C radioactivity in the alkaline traps was measured with a liquid scintillation counter (PerkinElmer Tri-Carb 2900TR). The analytical procedures have been described previously in [HERM et al., 2014; TAKAHASHI et al., 2014; YAMASHITA et al., 2014]. Table 4 presents the specific activity for Zircaloy-2.
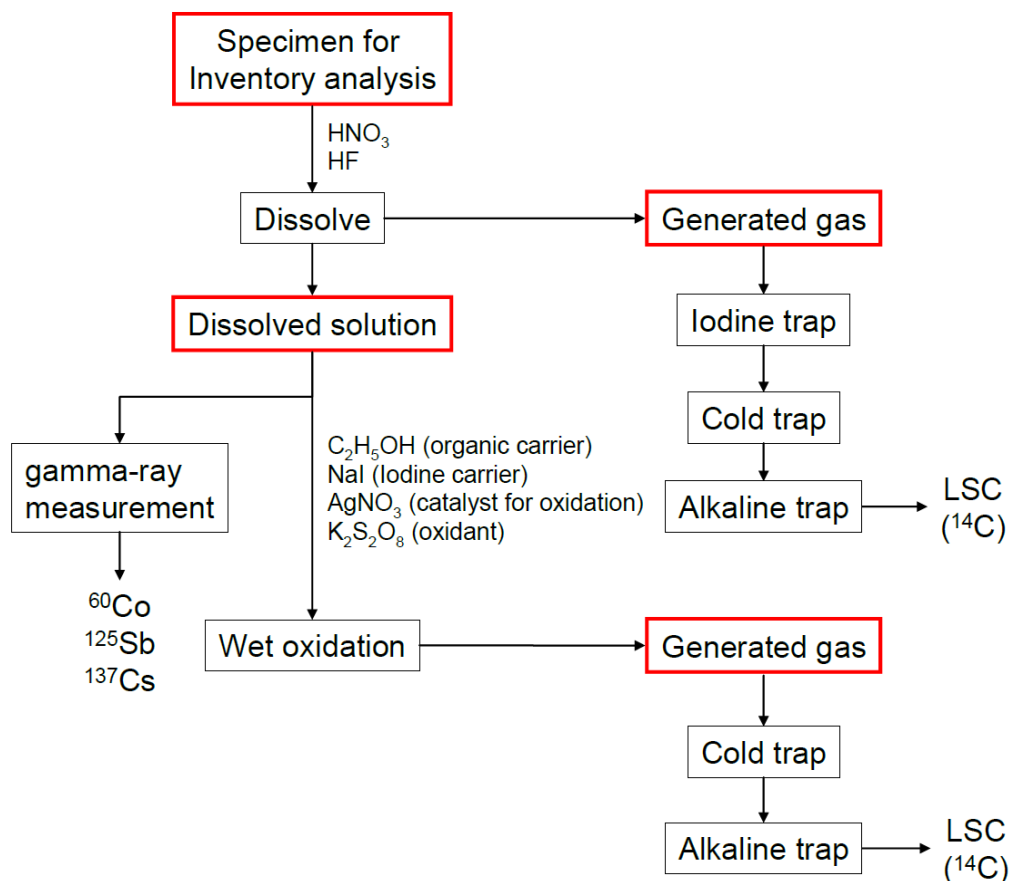

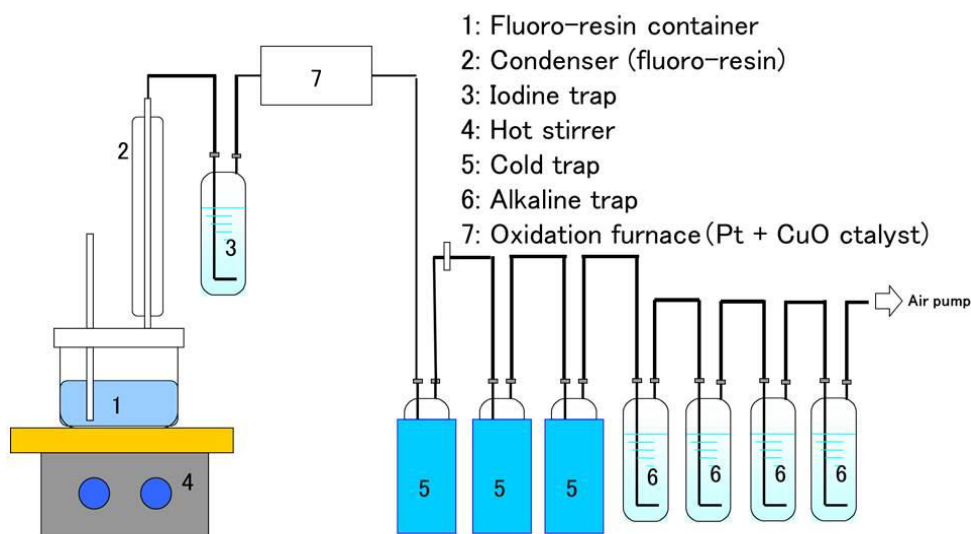**Figure 17 ^{14}C inventory analysis flow applied of irradiated Zircaloy-2 by digestion**

1: Fluoro-resin container
2: Condenser (fluoro-resin)
3: Iodine trap
4: Hot stirrer
5: Cold trap
6: Alkaline trap
7: Oxidation furnace (Pt + CuO ctalyst)

Figure 18 Outline of inventory measuring apparatus for quantification of ^{14}C of Zircaloy-2 specimens

Table 4 Specific radioactivity in irradiated Zircaloy-2 (Bq/g-Zr). The half-life corrections were made at a start of leaching test (mentioned in Section 3.2)

	C-14	Sb-125	Co-60	Cs-137
STEP I	2.48 x10^4	1.24 x10^6	2.07 x10^5	1.63 x10^6
STEP III	1.74 x10^4	1.04 x10^7	1.17 x10^6	4.95 x10^6

3.3 *Leached ^{14}C*

Corrosion tests as a static leaching tests were performed using a double vessel system as shown in Figure 19. The cladding of a 2 cm high cylinder polished with a 0.02 mm abrasive is immersed in a glass vial filled with 20 ml of NaOH solution adjusted to pH 12.5. The solution was deoxygenated before use to achieve an initial ORP (oxidation-reduction potential) of −253 mV. The glass vial was placed on the inside of a stainless steel container and sealed with a gasket to maintain the initial inert condition and to prevent leakage of volatile ^{14}C. This immersion procedure was carried out inside a simple glove box with a nitrogen atmosphere. The vessels were kept at room temperature of approximately 293 K. We prepared eight vessels containing irradiated claddings, seven of which were pretreated

and without the oxide layer and one with the oxide layer. The leaching test conditions are summarised in Table 5.

Figure 19 Vessels of corrosion test for irradiated Zricaloy-2.

Table 5 Experimental leaching conditions of Zircaloy-2 hulls in NaOH solution at pH 12.5

Sample No	Fuel cladding type	Leaching time, years	m/V (g/mL)
1	Zry2 STEP III, without oxide	0.5	0.29
2	Zry2 STEP III, without oxide	0.75	0.29
3	Zry2 STEP III, without oxide	1	0.29
4	Zry2 STEP III, without oxide	2	0.29
5	Zry2 STEP III, without oxide	3	0.29
6	Zry2 STEP III, without oxide	5.5	0.29
7	Zry2 STEP I, without oxide	5.5	0.39
8	Zry2 STEP I, with external oxide	6.5	0.20

After the test period, the released ^{14}C in the gas phase, and the partition of inorganic/organic ^{14}C in the liquid phase were determined for the whole procedure as shown in Figure 20. Figure 21 shows the procedure of gaseous total ^{14}C analysis in detail. The glove bag with a vacuum tube attached was filled up with air containing 0.25vol% of CO_2 before-hand. Outer

and inner containers were opened inside the glove bag. The gaseous ^{14}C was collected through the tube by using the three steps of an alkaline trap after passing through an oxidation furnace. ^{14}C collected in the alkaline traps was then liberated to the gaseous phase by addition of concentrated sulfuric acid, recollected in Carbosorb®, and measured using a liquid scintillation counter (PerkinElmer Tri-Carb 2900TR). From cold and tracer test results, the ^{14}C recovery rate of this method was about 87.2%.

Figure 22 shows the analysis for the dissolved ^{14}C. A portion of the liquid phase was provided for measurement of total dissolved ^{14}C as well as dissolved organic and inorganic ^{14}C. In the total ^{14}C measurement, an aliquot of leachate was mixed with a carrier carbon (Na_2CO_3 and C_2H_5OH), an oxidant (potassium persulfate, $K_2S_2O_8$), a catalyst ($AgNO_3$), and an acid (H_2SO_4) in a warm vessel. In the organic/inorganic separation method, first the inorganic ^{14}C was fractionated from another aliquot by bubbling for 30 minutes under acidification. After that, the remaining organics were oxidized with the same reagents used for total ^{14}C measurement and the volatile ^{14}C ($^{14}CO_2$) was collected by an alkaline trap in the same manner as described for total ^{14}C measurement. Leached ^{14}C in the alkaline traps was measured by a liquid scintillation counter (PerkinElmer Tri-Carb 3100TR). From cold and tracer test results, the ^{14}C recovery rates for respective fractions were over 93%.
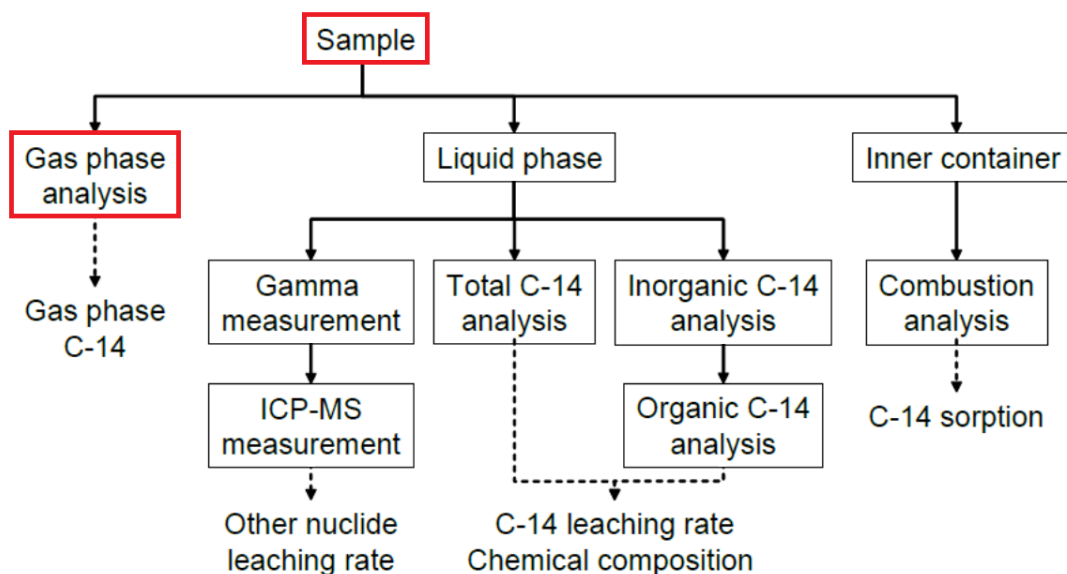

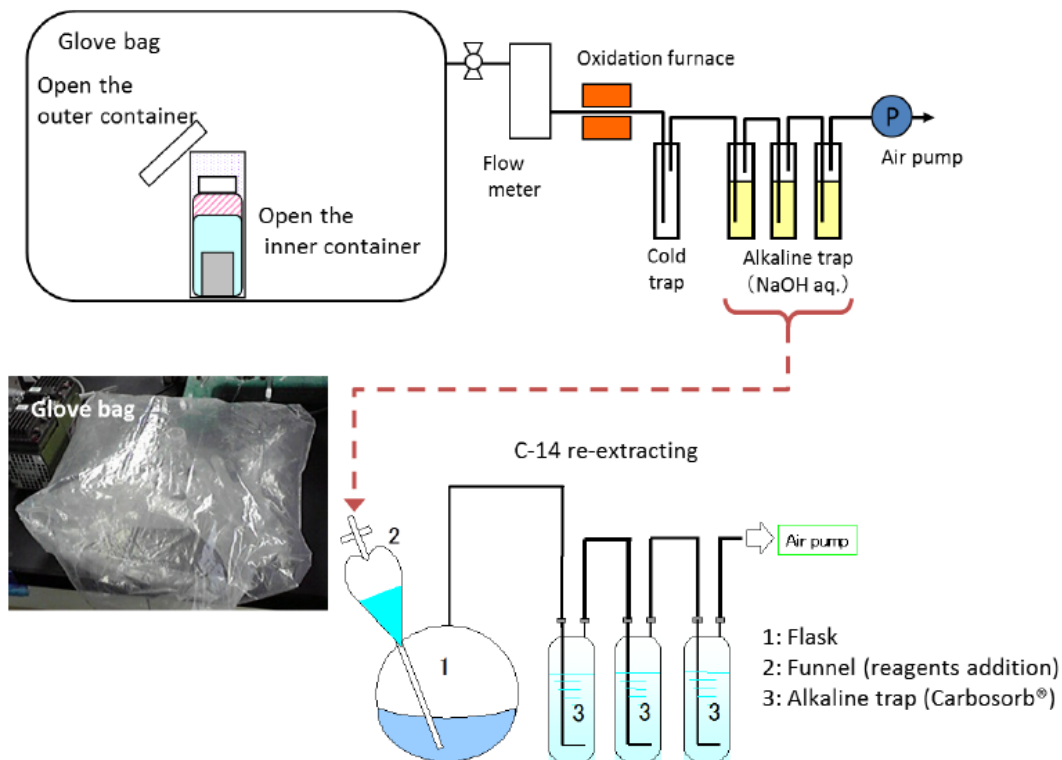**Figure 20 Analytical procedure of gaseous and dissolved organic/inorganic ^{14}C for the leaching test**

Figure 21 Outline of apparatus for gaseous total ^{14}C analysis

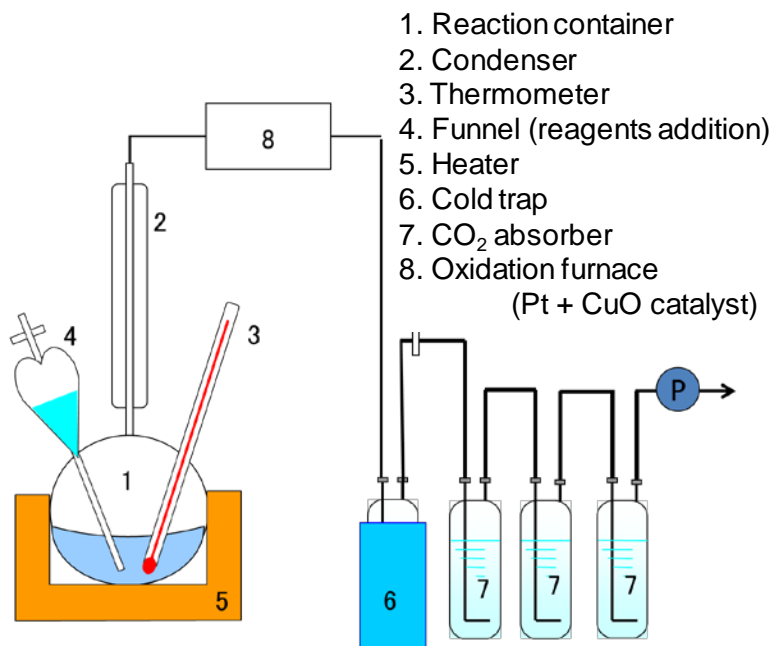1. Reaction container
2. Condenser
3. Thermometer
4. Funnel (reagents addition)
5. Heater
6. Cold trap
7. CO_2 absorber
8. Oxidation furnace
   (Pt + CuO catalyst)

Figure 22 Outline of apparatus for liquid ^{14}C analysis.

The total leached [14]C (gaseous and dissolved) from irradiated Zircaloy-2 without oxide has been calculated into equivalent corrosion rate and are described in a previous section (2.2 Corrosion Rate). Here, the leached ^{14}C for gaseous and dissolved organics/inorganics are discussed and shown in Figure 23. The total leached ^{14}C are in the order of 1- 2 Bq. The leached percentages for the respective fraction are summarised in Table 6. The results for the samples without the oxide layer (sample No 1-7) show a release of ^{14}C to gas and solution phases with a significant fraction released as gas (53-55%) during the first year. As the experiments continue, the fraction of ^{14}C released as gas decreases with time. In the dissolved fraction, the concentration of organics is higher than the inorganic one: the ratio organic/inorganic is approximately 2/3, except for the data at the test period of 1 year in which the total released ^{14}C was very low. For sample with an external oxide (sample No 8), the total leached ^{14}C is relatively higher than that for the sample without oxide. However, the leached fraction of ^{14}C in gas is relatively higher than that for the sample without oxide (16%), the overall trend is similar that the dissolved organic is major at 63%.
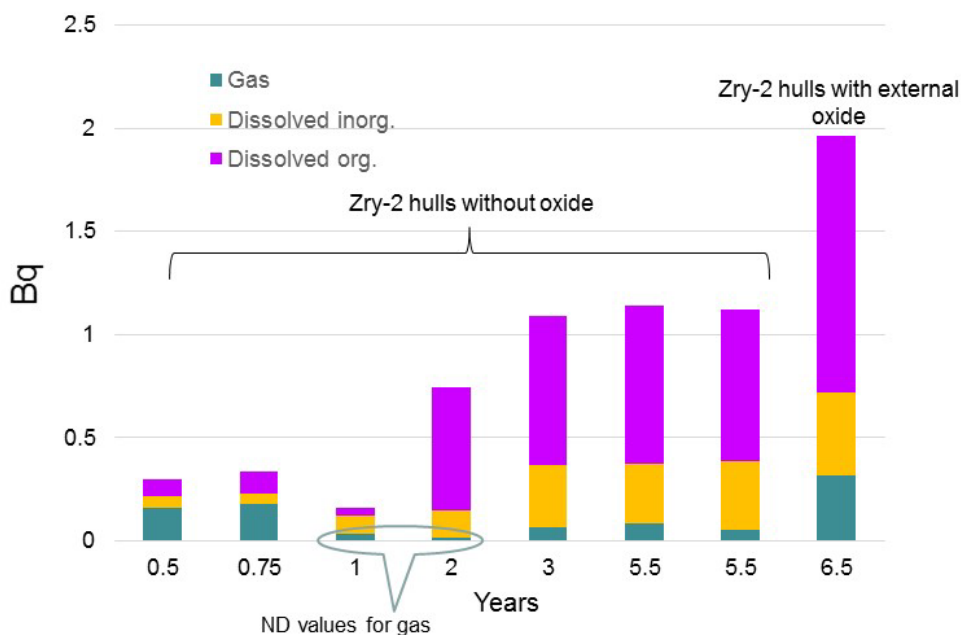

Figure 23 Leached ^{14}C and speciation in gas and liquid phases from irradiated Zircaloy-2.

Table 6 Fractions (%) of leached ^{14}C as gas, dissolved inorganics and organics

| Sample No	Fuel cladding type	years	Gas	Dissolved inorganics	Dissolved organics
1	Zry2 STEP III, without oxide	0.5	54.7	17.4	27.9
2	Zry2 STEP III, without oxide	0.75	52.8	16.5	30.6
3	Zry2 STEP III, without oxide	1	19.4*	58.6	21.9
4	Zry2 STEP III, without oxide	2	2.2*	17.8	80.0
5	Zry2 STEP III, without oxide	3	6.0	27.9	66.1
6	Zry2 STEP III, without oxide	5.5	7.4	25.0	67.6
7	Zry2 STEP I, without oxide	5.5	4.6	29.6	65.8
8	Zry2 STEP I, with external oxide	6.5	16.2	20.6	63.3

* Under the detection limit

3.4 *Instant Release Fraction (IRF)*

The instant release fraction (IRF) for hull waste is also discussed in the following section through the experiments using the irradiated Zircaloy-2 with external oxide. The release of radionuclides from the metal matrix is regarded as the corrosion-related congruent release. Conversely, the oxide film formed on the Zircaloy cladding surface is regarded as a source of IRF. In the preliminary Japanese safety case, 20% of ^{14}C in cladding was assumed as an IRF and the remaining 80% was assumed to be in the form of a corrosion-related congruent release from the base Zircaloy metal [FPEC/JAEA, 2007]. Therefore, the ^{14}C inventory in the oxide and the released ^{14}C from the oxide are of great importance. In order to investigate the IRF, the ^{14}C inventory in the oxide has been measured using irradiated cladding with a 25.3 μm thick external oxide film (Zircaloy-2, average rod burnup of 41.6 GWd/t_U) at first. Then, a static leaching test was carried out for 6.5 years using cladding tube whose internal oxide was removed. The major leaching source (oxide or base metal) is discussed in the following section.

As described earlier in section 3.2, a spent BWR fuel rod (STEP I type) was prepared. After the fuel components were removed, the claddings were washed with HNO_3 in a warm bath and cut to an appropriate size. The thickness of the surface oxide layer was measured based on external observations. As shown in Figure 24, four types of samples were obtained for specific activity measurements of ^{14}C. The external oxide layer of Zircaloy was peeled off through vertical compression of the columnar cladding (approximately 2 cm high) whose interior layer had previously been removed. As a consequence, approximately 0.05 g of oxide was recovered as a powdery fragment.

The ^{14}C radioactivity in the cladding specimens was measured as described in section 3.2. First, the ring-shaped claddings and oxide samples were dissolved in an HNO_3 + HF solution and then heated. Carbon components were evaporated by air bubbling for 30 min and oxidized by CuO in CO_2 at 1073 K. The material was then passed through three steps of a dry-ice cold trap to remove tritium and three steps of an alkaline trap (1 M of NaOH) to collect carbon dioxide ($^{14}CO_2$). The ^{14}C radioactivity in the alkaline traps was measured with a liquid scintillation counter (PerkinElmer Tri-Carb 2900TR).
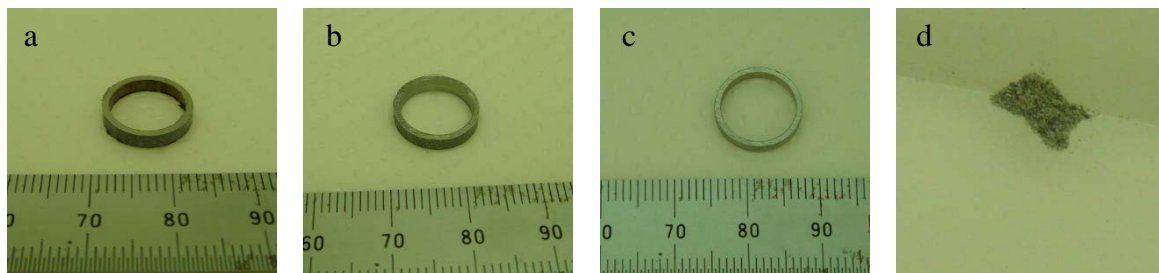
Figure 24 Photographs showing irradiated Zr claddings: (a) with internal and external oxide layers in place, (b) with internal oxide removed, (c) with internal and external oxide removed, (d) (external) oxide fragment removed from the cladding [Sakuragi et al., 2016b].

The results of ^{14}C measurement are summarized in Table 7. The specific activity (Bq/g) between oxide and base Zircaloy differs by a factor of 2.8. This may be due to the additional activation reaction of $^{17}O(n,\alpha)^{14}C$ in oxide together with the $^{14}N(n,p)^{14}C$ reaction. However, the abundance of ^{14}C in the oxide and the base Zircaloy, which is obtained from cladding geometry, can be estimated as 7.5% and 92.5%, respectively. This ^{14}C distribution

27

corresponds roughly to the ^{14}C inventory in waste claddings estimated by the ORIGEN calculation in previous work [SAKURAGI *et al.*, 2013], in which the respective percentages of 3.5% and 96.5% were suggested for the BWR cladding. It can therefore be concluded from the results of both the measurements in this study and previous calculations that the assumption of 20% IRF as has been used in some safety case studies [FPEC/JAEA, 2007] is conservative; a lower IRF is justified in the work reported herein. However, the ^{14}C distribution in oxide for the PWR cladding was measured as 17% [YAMAGUCHI *et al.*, 1999], which was used as a basis for the Japanese report. This can be attributed to the oxide thickness of the claddings and that the oxide layer of PWR cladding in the literature is especially thick at 80 µm.

Table 7 Specific activity of ^{14}C for irradiated Zircaloy and oxide [Sakuragi et al., 2016b].

Thickness (*µm*)		Specific activity (*Bq/g*)			
Base metal	Oxide layer	(a) Cladding with internal and external oxide	(b) Cladding with external oxide	(c) Cladding base metal	(d) External oxide*
704.7	25.3	1.54×10^4 1.49×10^4 1.43×10^4	1.53×10^4	1.49×10^4 1.50×10^4 1.47×10^4	4.25×10^4 3.83×10^4

* Units of grams in the oxide are converted to grams of zirconium, not grams of ZrO_2.

The static leaching test was carried out using the irradiated Zircaloy-2 cladding, described above (section 3.3, sample No 8), of a 2 cm high cylinder with an external oxide layer but with its internal oxide layer removed. The sample was immersed in NaOH solution adjusted to a pH of 12.5 and kept 6.5 years under room temperature around 293 K. The leaching test is shown in Figure 25. The leached ^{14}C was measured as in section 3.3.

Figure 25 External view of the outer vessel (left) and cladding with external oxide immersed in the glass vessel (right) for long-term static leaching tests.

Table 8 shows the results of the leached ratio of ^{14}C after 6.5 years of aqueous immersion. The leaching ratio, which represents the leached amount (gaseous + dissolved) divided by the initial inventory, is very low (0.0038%). The results for the respective fractions have already been presented and discussed in section 3.3.

In order to investigate the release mechanisms, ^{14}C based studies were conducted on the assumption that the radionuclide release from the Zircaloy matrix is congruent with corrosion. The immersed cladding in this study comprises the external oxide layer and bare Zircaloy metal inside the tube. Therefore, the potential leaching source can be divided among three surfaces: (a) interior bare Zircaloy ($r_{in\text{-}Zry}$), (b) external Zircaloy and oxide interface ($r_{out\text{-}Zry}$), and (c) external oxide layer ($r_{out\text{-}oxide}$). The ^{14}C released from the oxide layer can be expressed from the total release of ^{14}C (r_{total}) obtained experimentally, as

$$r_{out-oxide} = r_{total} - r_{in-Zry} - r_{out-Zry} \qquad (10)$$

The matrix corrosion rate was obtained from out-of-pile study in the temperature range of approximately 561 K to 673 K [HILLNER, 1977]. Here, the pre-transition cubic rate constant, k_C, is applied to the inside bare Zircaloy (r_{in-Zry}) and the post-transition linear rate constant, k_L, is applied to the external Zircaloy ($r_{out-Zry}$) because the corrosion kinetics of Zircaloy follows a cubic rate law before the transition ("breakaway"). Beyond 2 µm for the oxide thickness, the corrosion kinetics changes linearly with time [HILLNER, 1977]. The details for equation (10) are described elsewhere [SAKURAGI *et al.*, 2016b].

Figure 26 shows the estimated release ratios from the possible source surfaces at 293 K and 6.5 years of immersion. Due to the low corrosion rate of Zircaloy, especially the extremely slow post-transition corrosion kinetics, the leached ^{14}C from Zircaloy is negligible. This leads to the conclusion that the main source of ^{14}C release is from the oxide. By applying the concept of a corrosion-related congruent release described above, the ^{14}C release from the oxide layer is almost 100% of the amount in the previous short-term PWR test [YAMAGUCHI *et al.*, 1999], for which the cladding has both post-transition internal and external oxide layers of 10 µm and 80 µm respectively.

Table 8 Results of released ^{14}C from irradiated Zircaloy-2 hull with external oxide after 6.5 years of aqueous immersion [Sakuragi et al., 2016b].

Initial inventory, $A_{inventory}$	Gas phase	Total dissolved	Leaching ratio
6.17×10^4 Bq	0.317 Bq	2.00 Bq	0.0038%
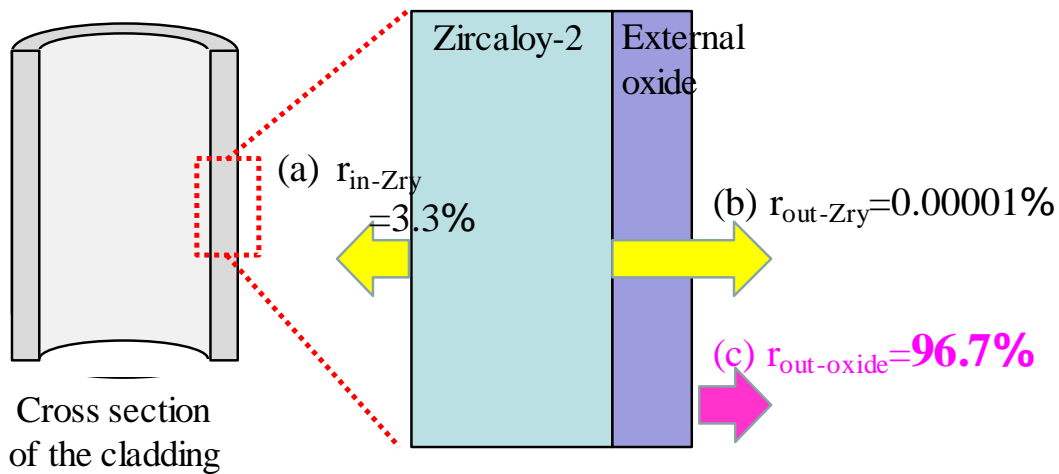
Figure 26 Estimated leached ^{14}C from the oxide based on the corrosion-related congruent release.

Based on the assumption made in the previous paragraph, the main source of ^{14}C release is from the oxide. However, regarding the ^{14}C in the oxide as an IRF would be overly conservative, because the total leached ^{14}C from the hull with oxide is 0.0038% after 6.5 years of immersion as mentioned before. The results of leaching tests are shown in Figure 27, together with the results for irradiated Zircaloy-2 and Zircaloy-4 [YAMAGUCHI *et al.*, 1999] with and without oxide. The previous short-term leaching tests for PWR hulls with inner and external oxide also showed small leaching ratios less than 0.03% [YAMAGUCHI *et al.*, 1999]. Both the low amount of ^{14}C in the oxide and as well as low leaching rate indicate that the ^{14}C in the oxide does not have a major impact on the instant release fraction; this understanding should be reflected in the safety case. If not instant release, other mechanisms need to be taken into consideration to explain ^{14}C release from the oxide. For example, the solubility of zirconia under deep disposal conditions is a challenge that needs to be addressed bearing in mind that the solubility of zirconia is extremely low in alkaline media.
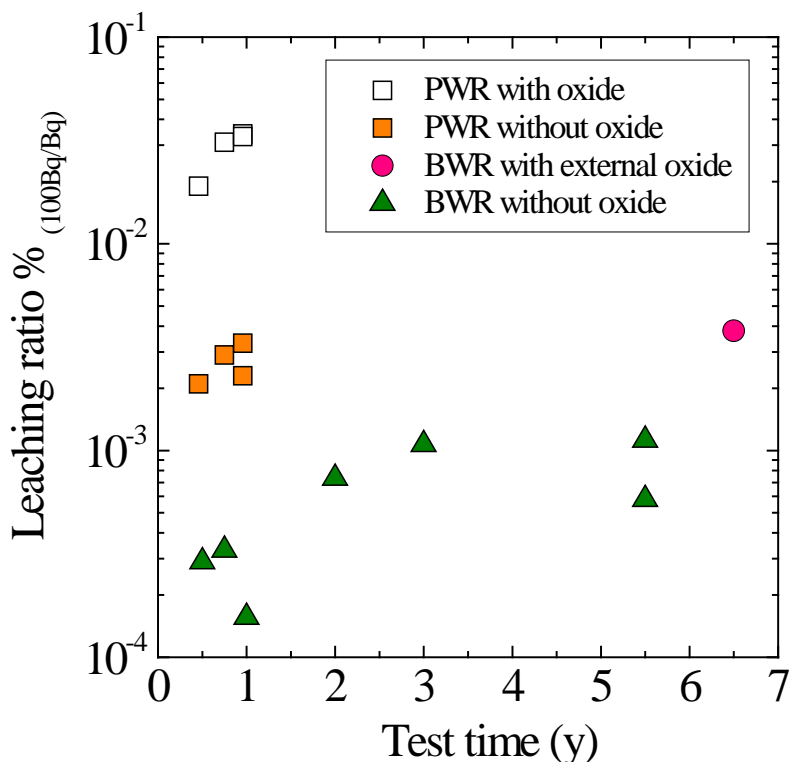
Figure 27 Leached ^{14}C from irradiated Zr claddings: PWR with oxide (white square), PWR without oxide (orange square) [Yamaguchi et al., 1999], BWR without oxide (green triangle), and BWR with external oxide (pink circle) [Sakuragi et al., 2016b].

4   Conclusion

Corrosion tests for unirradiated and irradiated Zr alloys were performed. The corrosion rates of unirradiated Zr alloys were very low, decreased with time and increased as the temperature increased. The rise in pH slightly increased the corrosion rate, but the influence of other chemical components of the solution on the rate was not significant. The equivalent corrosion rate of irradiated Zircaloyo-2 obtained from leached ^{14}C assumed congruence with corrosion was less than that of unirradiated Zircaloy. Since this cannot be sufficiently explained with only the difference of the test condition (temperature), the congruence of ^{14}C leaching with corrosion has not been confirmed yet and is a future challenge.

 In the corrosion tests for irradiated Zircaloy-2 (spent BWR cladding), the concentrations of released ^{14}C as gaseous and dissolved organics and inorganics were measured. The gaseous

[14]C fraction decreased with time from 53-55% to 7%. By contrast, the fraction of ^{14}C in liquid phase increased with time. In the dissolved fraction, the organics is higher than the inorganics one: the ratio organic/inorganic is approximately 2/3.

Instant release fraction (IRF) for spent claddings was also discussed through the experiment with the leached ^{14}C ratio from irradiated Zircaloy-2 having an oxide film and the ^{14}C inventory of the oxide part. The inventory measurement found that the abundance of ^{14}C in the oxide was only 7.5%, which is less than the 20% estimated in the safety case. Further, the leached ^{14}C from the irradiated cladding with the oxide was found to be 0.0038% of the total ^{14}C activity after 6.5 years of immersion. These understandings should be reflected in the safety case that a lower IRF is justified or a negligible IRF is potentially suggested.

Acknowledgement

References

International Atomic Energy Agency (IAEA), 1998. Durability of Spent Nuclear Fuels and Facility Components in Wet Strage, IAEA-TECDOC-1012, Vienna.

FRANKER, A. C. and HARRIS, J. S. 1990. Corrosion Behavior of Zirconium Alloy Nuclear Fuel Cladding, *Mat. Res. Soc. Symp. Proc*. 176, 549.

Federation of Electric Power Companies (FEPC) and Japan Atomic Energy Agency (JAEA) 2007, Second Progress Report on Research and Development for TRU Waste Disposal in Japan, JAEA AND FEPC REPORT TRU-2.

GUENTHER, R.J., BLAHNIK, D.E., THOMAS, L.E., BALDWIN, D.L., MENDEL, J.E. 1990. Radionuclide distribution in LWR spent fuel. Proc. Spectrum 90 Conference, Sept. 30-Oct.3, Knoxville, TN 1990.

HERM, M., TANABE, H., SAKURAGI, T., TATEISHI, T., YAMASHITA, Y., BOTTLE, M., GONZALES-ROBLES, E., KIENZLER, B., BOTTOMLEY, P. D. W., SERRANO-PURROY, D., WEGEN., D. H. and METZ., V. 2014. Description of the analytical procedure for gaseous and dissolved C-14 species quantification. *CAST Project*. CASTWP3 - D.3.3.

HILLNER, E. 1977. Corrosion of zirconium-base alloys–An overview, *Zirconium in the Nuclear Industry, 3rd Int. Symp., ASTM STP* 633, 211-235.

HONDA, A. NISHIMURA, T., WADA, R., TANABE, M. 1999. Long Term Testing System, Testing Container and Measurement Container, Japan Patent 2912365.

KATO, O., TANABE, H., SAKURAGI, T., NISHIMURA, T., TATEISHI, T. 2014. Corrosion tests of Zircaloy hull waste to confirm applicability of corrosion model and to evaluate influence factors on corrosion rate under geological disposal conditions, *Mater. Res. Soc. Symp. Proc.* 1665, 195-202.

SAKURAGI, T., MIYAKAWA, H., NISHIMURA, T., TATEISHI, Y. 2012. Corrosion Rates of Zircaloy 4 by Hydrogen Measurement under High pH, Low Oxygen and Low Temperature Conditions, *Mater. Res. Soc. Symp. Proc.* 1475, 311-316.

SAKURAGI, T., TANABE, H., HIROSE, M., SAKASHITA, A., NISHIMURA, T. 2013. Estimation of Carbon 14 Inventory in Hull and End-Piece Wastes from Japanese Commercial Reprocessing Operation, *Proceedings of the ICEM2013*. Brussels, Belgium.

SAKURAGI, T. in prep. Report on corrosion behaviour of stainless steel (D2.12), CAST Project Report.

SAKURAGI, T., YOSHIDA, S., KATO, O., TATEISHI, Y. 2016a. Study of stainless steel corrosion by hydrogen measurement under deoxygenated, low-temperature and basic repository conditions. *Progress in Nuclear Energy* 87, 26-31.

SAKURAGI, T., YAMASHITA, Y., AKAGI, M., and TAKAHASHI, Y. 2016b. Carbon 14 distribution in irradiated BWR fuel cladding and released carbon 14 after aqueous immersion of 6.5 years, *Procedia Chemistry, Proceedings of the 5th International ATALANTE Conference on Nuclear Chemistry for Sustainable Fuel Cycles.*.

SAKURAGI, T, MIYAKAWA, H, NISHIMURA, T, TATEISHI, T. 2013. Long-term corrosion of Zircaloy-4 and Zircaloy-2 by continuous hydrogen measurement under repository condition, *Mater. Res. Soc. Symp. Proc.* 1518, 173-178.

SHOESMITH, D.W., ZAGIDULIN, D. 2011. The corrosion of zirconium under deep geologic repository conditions, *J Nucl Mater* 418, 292-306.

TAKAHASHI, R., SASOH, M., YAMASHITA, Y., TANABE, H. SAKURAGI, T. 2014. Improvement of inventory and leaching rate measurements of C-14 in hull waste, and separation of organic compounds for chemical species identification, *Mater. Res. Soc. Symp. Proc.* 1665, 139-148.

YAMAGUCHI, T., TANUMA, S., YASUTOMI, I., NAKAYAMA, T., TANABE, H., KATSURAI, K., KAWAMURA, W., MAEDA, K., KITAO, H., SAIGUSA, M. 1999. A study on chemical forms and migration behavior of radionuclides in hull waste, *Proc. 7th International Conference on Environmental Remediation and Radioactive Waste Management, ICEM1999*, Nagoya, Japan.

YAMASHITA, Y., TANABE, H., SAKURAGI, T., TAKAHASHI, Y., SASOH, M. 2014. C-14 release behavior and chemical species from irradiated hull waste under geological disposal conditions, *Mater. Res. Soc. Symp. Proc.*, Vol. 1665, 187-194.